

A Reduced Scheme Based on POD for a Convection-Diffusion Boundary Control Problem with Control/State Constraints

Guoping Zhang, Xianbing Luo

College of Mathematics and Statistics, Guizhou University, Guiyang, P.R. China

Email address

zygpzhang@126.com (Guoping Zhang)

Citation

Guoping Zhang, Xianbing Luo. A Reduced Scheme Based on POD for a Convection-Diffusion Boundary Control Problem with Control/State Constraints. *Computational and Applied Mathematics Journal*. Vol. 4, No. 4, 2018, pp. 57-64.

Received: December 15, 2018; Accepted: January 3, 2019; Published: January 19, 2019

Abstract: To solve a problem of high real-time performance and large computational complexity in two-dimensional convection-diffusion boundary control problem with constraints, an optimal real-time control method based on reduced order model with constraints is proposed. Using proper orthogonal decomposition (POD) of snapshot, we first obtain a reduced finite difference scheme. Then, a quadratic programming method with constraints single-step rolling optimization algorithm (CSROA) is adopted and verified with improved saturated linear quadratic regulator (ISLQR) controller. Finally, to verify the validity and accuracy of the proposed method, numerical simulations are presented.

Keywords: Convection-Diffusion, Boundary Control, POD

1. Introductions

Convection-diffusion optimal control problem is widely used in environmental science, chemical reaction and other fields [1-8]. In real control problems, the state variable, the input variable (control variable) and the output variable is almost all constrained. So whether the optimal control method can be widely used in practical problems or not depends on our ability to deal with constraints [9-11]. Therefore, it is significant to find stable and high efficient numerical methods. Finite difference method is a common method to solve the convection-diffusion optimal control problem with constraints. Generally, the computational cost of these problems are very high. How to simplify the calculations, reduce the computing time and ensure the solution has sufficient accuracy are particularly important works.

The POD method based on matrix singular value

decomposition (SVD) is widely used because of its ability to provide low-order models with high accuracy and small degrees of freedom. It is a good numerical method which can effectively approximate a large number of data, [12-17]. Its essence is to find an orthogonal basis which can represent the given data in the sense of least square.

For the convection-diffusion reaction process, the optimal control of the linear quadratic regulator (LQR) based on the low-order model without constraints is designed by Li et al. [18]. The dimension of the discrete space is reduced, and the real-time application of the optimal feedback control is simulated. To our knowledge, there is no result for a two-dimensional unsteady convection-diffusion boundary control problem with control/state constraints.

In this paper, the following initial boundary value problems are considered for two-dimensional unsteady convection-diffusion boundary control problems:

$$\begin{aligned} \frac{\partial U}{\partial t} + v_1 \frac{\partial U}{\partial x} + v_2 \frac{\partial U}{\partial y} &= D \left(\frac{\partial^2 U}{\partial x^2} + \frac{\partial^2 U}{\partial y^2} \right), x \in [a, b], y \in [c, d], t \in [0, T], \\ \frac{\partial U}{\partial x}(a, y, t) &= \frac{\partial U}{\partial x}(b, y, t) = 0, U(x, c, t) = u(x, t), U(x, d, t) = 0, \\ U(x, y, 0) &= 0, \end{aligned} \quad (1)$$

where $U(x, c, t) = u(x, t)$ represents the input variable, $\frac{\partial U}{\partial x}(b, y, t) = 0$ represents the output variable, D represents the coefficient of fluid diffusion, v_1 and v_2 are the flow velocity of the fluid in the reactor, respectively. The objective function J is the following:

$$\min_{u(t)} J = \int_0^{\infty} [y(t) - y_f]^2 dt + \delta^2 \int_0^{\infty} [u(t) - u_f]^2 dt, \quad (2)$$

where $\delta > 0$ is the weight of the control action, y_f and u_f represent steady-state value of output and input of the control process, respectively.

The POD basis is obtained through the SVD of snapshots, which transforms the discrete higher order state space into low order model with good precision. Then the quadratic programming method with CSROA is adopted and verified with ISLQR controller. The numerical results show that the computation speed can be greatly improved under the same accuracy of the optimization results.

$$\begin{aligned} \sigma_x^- U_{i,j}^n &= \frac{1}{h_x} (U_{i,j}^n - U_{i-1,j}^n) \text{ for } v_1 \geq 0; & \sigma_x^+ U_{i,j}^n &= \frac{1}{h_x} (U_{i+1,j}^n - U_{i,j}^n) \text{ for } v_1 < 0; \\ \sigma_y^- U_{i,j}^n &= \frac{1}{h_y} (U_{i,j}^n - U_{i,j-1}^n) \text{ for } v_2 \geq 0; & \sigma_y^+ U_{i,j}^n &= \frac{1}{h_y} (U_{i,j+1}^n - U_{i,j}^n) \text{ for } v_2 < 0; \\ \sigma_x^2 U_{i,j}^n &= \frac{1}{h_x^2} (U_{i+1,j}^n - 2U_{i,j}^n + U_{i-1,j}^n); & \sigma_y^2 U_{i,j}^n &= \frac{1}{h_y^2} (U_{i,j+1}^n - 2U_{i,j}^n + U_{i,j-1}^n). \end{aligned}$$

Then, the discrete form of (1) can be expressed as

$$U_{i,j}^{n+1} = A_0 U_{i,j}^n + A_1 U_{i+1,j}^n + A_2 U_{i,j+1}^n + A_3 U_{i-1,j}^n + A_4 U_{i,j-1}^n, \quad (3)$$

where

$$\begin{aligned} A_0 &= 1 - \tau \left(\frac{|v_1|}{h_x} + \frac{|v_2|}{h_y} \right) - \left(\frac{2D\tau}{h_x^2} + \frac{2D\tau}{h_y^2} \right), & A_1 &= -\tau \frac{v_1 - |v_1|}{2h_x} + \frac{D\tau}{h_x^2}, \\ A_2 &= -\tau \frac{v_2 - |v_2|}{2h_y} + \frac{D\tau}{h_y^2}, & A_3 &= \tau \frac{v_1 + |v_1|}{2h_x} + \frac{D\tau}{h_x^2}, & A_4 &= \tau \frac{v_2 + |v_2|}{2h_y} + \frac{D\tau}{h_y^2}. \end{aligned}$$

Note that

$$\begin{aligned} \mathbf{x}(k) &= (U_{1,2}^k, U_{2,2}^k, \dots, U_{m,2}^k, U_{m+1,2}^k, U_{1,3}^k, U_{2,3}^k, \dots, U_{m,3}^k, U_{m+1,3}^k, \dots, U_{1,m}^k, U_{2,m}^k, \dots, U_{m,m}^k, U_{m+1,m}^k)^*, \\ y(k) &= U_{m+1,j}^k, j = 2, 3, \dots, m, \\ \mathbf{B} &= [A_4, A_4, \dots, A_4, 0, \dots, 0, \dots, 0, \dots, 0]^*, \quad \mathbf{c} = [0, 0, \dots, 1, 0, 0, \dots, 1, \dots, 0, \dots, 1]. \end{aligned}$$

Then formula (3) can be sorted into the following discrete higher-order state space model

$$\begin{cases} \mathbf{x}(k+1) = \mathbf{A}\mathbf{x}(k) + \mathbf{B}u(k), \\ y(k) = \mathbf{c}\mathbf{x}(k), \end{cases} \quad (4)$$

where

2. Reduced Algorithm

2.1. Finite Difference method For Initial Boundary Value Problems

In order to discuss the difference scheme, the time interval $[0, T]$ is divided into N equal partitions, the length of each partition is $\tau := T/N$, time $t_n = n\tau$, and the terminal time is expressed as $t(N)$, $n = 0, 1, 2, \dots, N$. Grid points are represented as (x_i, y_j, t_n) , where $x_i = a + ih_x$, $y_j = c + jh_y$, h_x, h_y are space steps and $i, j = 1, 2, \dots, m+1$.

Let

$$\sigma_t U_{i,j}^{n+1} = \frac{1}{\tau} (U_{i,j}^{n+1} - U_{i,j}^n),$$

and

$$\mathbf{A} = \begin{bmatrix} \mathbf{G}_{m+1} + \mathbf{I}_{m+1} & \mathbf{A}_2 \mathbf{I}_{m+1} & & & \\ \mathbf{A}_4 \mathbf{I}_{m+1} & \ddots & & & \\ & \ddots & \ddots & & \\ & & \ddots & \mathbf{A}_2 \mathbf{I}_{m+1} & \\ & & & \mathbf{A}_4 \mathbf{I}_{m+1} & \mathbf{G}_{m+1} + \mathbf{I}_{m+1} \end{bmatrix} \in \mathbb{R}^{(m-1)(m+1) \times (m-1)(m+1)},$$

$\mathbf{I}_{m+1} \in \mathbb{R}^{(m+1) \times (m+1)}$ is the unit matrix and \mathbf{G}_{m+1} is defined as

$$\mathbf{G}_{m+1} = \begin{bmatrix} A_0 + A_3 & A_1 & & & \\ & A_3 & A_0 & & \\ & & \ddots & & \\ & & & \ddots & \\ & & & & A_0 & A_1 \\ & & & & A_3 & A_0 + A_1 \end{bmatrix} \in \mathbb{R}^{(m+1) \times (m+1)}.$$

2.2. POD Method

The snapshots calculated by the above finite difference method can be expressed as a matrix $\mathbf{U} \in \mathbb{R}^{(m-1)(m+1) \times d}$:

$$\mathbf{U} := (\mathbf{u}_{n_1}, \mathbf{u}_{n_2}, \dots, \mathbf{u}_{n_d}), \tag{5}$$

where

$$\mathbf{u}_{n_l} = (U_{1,2}^{n_l}, U_{2,2}^{n_l}, \dots, U_{m+1,2}^{n_l}, U_{1,3}^{n_l}, U_{2,3}^{n_l}, \dots, U_{m+1,3}^{n_l}, \dots, U_{1,m}^{n_l}, U_{2,m}^{n_l}, \dots, U_{m+1,m}^{n_l})^T,$$

and $l = 1, 2, \dots, d$.

Define the matrix norm $\|\cdot\|_{\xi, \eta}$ as

$$\|\mathbf{A}\|_{\xi, \eta} = \sup_{\mathbf{x} \neq 0} \frac{\|\mathbf{A}\mathbf{x}\|_{\xi}}{\|\mathbf{x}\|_{\eta}}.$$

Then the optimization problem of \mathbf{U} is to obtain the corresponding $\Phi = \{\phi_1, \phi_2, \dots, \phi_d\} \in \mathbb{R}^{(m-1)(m+1) \times d}$, such that

$$J(\Phi) = \|\mathbf{U} - \Phi\Phi^T \mathbf{U}\|_{2,2} \tag{6}$$

is minimized, where $d \ll N$ and Φ is defined as the set of all normal orthogonal basis in \mathbb{R}^d .

The SVD of matrix $\mathbf{U} \in \mathbb{R}^{(m-1)(m+1) \times d}$ is as follows:

$$\mathbf{U} = \mathbf{W}\mathbf{S}\mathbf{V}^T = \mathbf{W} \begin{bmatrix} \mathbf{S}_j & 0 \\ 0 & 0 \end{bmatrix} \mathbf{V}^T,$$

Where $\mathbf{W} \in \mathbb{R}^{(m-1)(m+1) \times (m-1)(m+1)}$, $\mathbf{V} \in \mathbb{R}^{d \times d}$. \mathbf{W} and \mathbf{V} are orthogonal matrices, $\mathbf{S}_j = \text{diag}\{\lambda_1, \lambda_2, \dots, \lambda_j\} \in \mathbb{R}^{j \times j}$ is diagonal matrix corresponding to \mathbf{U} , and $\lambda_1 \geq \lambda_2 \geq \dots \geq \lambda_j \geq 0$.

From the relation between the spectral radius and the $\|\cdot\|_{2,2}$

$$\|\alpha^l - \mathbf{P}_M(\alpha^l)\|_2 = \|(\mathbf{U} - \mathbf{U}_M)\delta_l\|_2 \leq \|\mathbf{U} - \mathbf{U}_M\|_{2,2} \|\delta_l\|_2 = \sqrt{\lambda_{M+1}}, \tag{8}$$

Where $\mathbf{P}_M(\alpha^l) = \sum_{j=1}^M (\phi_j, \alpha^l) \phi_j$, and (ϕ_j, α^l) is the standard inner product of vectors ϕ_j and α^l . Inequality

norm, one can get that if a number $M < r$, $r(r \leq j \leq d)$ is the rank of the matrix \mathbf{U} , then the following equation holds

$$\lambda_{M+1} = \min_{\text{rank}(\mathbf{B}) \leq M} \|\mathbf{U} - \mathbf{B}\|_{2,2} = \|\mathbf{U} - \mathbf{U}_M\|_{2,2}, \tag{7}$$

Where $\mathbf{U}_M = \sum_{i=1}^M \lambda_i \phi_i \phi_i^T$, $i = 1, 2, \dots, M$. ϕ_i and ϕ_i are

the i -th column vectors of matrix \mathbf{W} and \mathbf{V} , respectively.

Through equations (6) and (7), one can obtain that the minimum distance between \mathbf{U} and \mathbf{B} ($\text{rank}(\mathbf{B}) = M$) is equivalent. That is, \mathbf{U}_M is the optimal expression of \mathbf{U} by \mathbf{B} , which is defined in (7), and \mathbf{U}_M is the optimal representation of \mathbf{U} in the optimal basis. Then, one can get that $\Phi = \mathbf{W}_M = (\phi_1, \phi_2, \dots, \phi_d)$ ($M \ll d$) is the optimal basis of the optimization problem (6).

Set the d column vectors of \mathbf{U} be $u_{n_j} = \alpha^l$ and δ_l denotes column unit vector with one component of 1 and the rest of 0, $l = 1, 2, \dots, d$. By the compatibility of vector norm and the matrix norm, then

(8) shows that $\mathbf{P}_M(\alpha^l)$ is the optimal approximation of α^l , and the error is $\sqrt{\lambda_{M+1}}$.

Next, we use the optimal basis to construct a simplified

difference scheme. Projecting the model (4) into the reduced order space generated by the POD basis function, then

$$\begin{cases} \mathbf{x}(k) \approx \Phi \alpha(k), \\ \alpha(k) \approx \Phi^* \mathbf{x}(k). \end{cases} \quad (9)$$

Submitting (9) into (4), we obtain

$$\begin{cases} \Phi^{\text{th}} \Phi \alpha(k+1) = \Phi \mathbf{A} \Phi \alpha(k) + \Phi^2 \mathbf{B} u(k), \\ y(k) = \mathbf{c} \Phi \alpha(k). \end{cases}$$

Further, by $\Phi^* \Phi = \mathbf{I}$, then

$$\begin{cases} \alpha(k+1) = \mathbf{A}_r \alpha(k) + \mathbf{B}_r u(k), \\ y(k) = \mathbf{c}_r \alpha(k), \end{cases} \quad (10)$$

where $\mathbf{A}_r = \Phi^* \mathbf{A} \Phi$, $\mathbf{B}_r = \Phi^* \mathbf{B}$, and $\mathbf{c}_r = \mathbf{c} \Phi$.

By iterative computation, one can obtain $\alpha(k)$ ($k=1,2,\dots,N$) by solving M equations in (10), where $M \ll (m-1)(m+1)$. The approximate solution $\mathbf{x}(k) = \Phi \alpha(k)$ of model (1) can be obtained by using the optimal basis Φ .

If the full order model (4) is used, $(m-1)(m+1)$ equations need to be solved in every iteration. However, to get the approximate solution on the problem, we need to solve only few equations by using the method of reduced order model (10). Thus, the reduced order model greatly reduces the degree of freedom, saves the computer memory, and shortens the computing time.

3. Solution of optimal Control

3.1. Optimal Control of Full-Order Model

Described in terms of the discretization model of (4), the objective function J in (2) can be written in the following form

$$\min_{\tilde{u}} J = \sum_0^{\infty} (\tilde{\mathbf{x}}^* \mathbf{Q} \tilde{\mathbf{x}} + \tilde{u}^* R \tilde{u}),$$

subject to

$$\begin{cases} \tilde{\mathbf{x}}(k+1) = \mathbf{A} \tilde{\mathbf{x}}(k) + \mathbf{B} \tilde{u}(k), \\ \tilde{y}(k) = \mathbf{c} \tilde{\mathbf{x}}(k), \end{cases} \quad (11)$$

where $\mathbf{Q} = \mathbf{c}^* \mathbf{c}$, $R = \delta^2$, $\tilde{\mathbf{x}} = \mathbf{x} - \mathbf{x}_f$, $\tilde{u} = u - u_f$.

The optimal can be expressed as $\tilde{u}(k) = -\mathbf{L} \tilde{\mathbf{x}}(k)$, $\mathbf{L} \in \mathbb{R}^{1 \times (m-1)(m+1)}$ is a constant feedback gain matrix, expressed as

$$\mathbf{L} = (\mathbf{R} + \mathbf{B}^{\text{th}} \mathbf{K} \mathbf{B})^{-1} \mathbf{B}^* \mathbf{K} \mathbf{A},$$

where the parameter \mathbf{K} is determined by the algebraic Riccati equation

$$-\mathbf{K} + \mathbf{Q} + \mathbf{A}^{\text{th}} \mathbf{K} \mathbf{A} - \mathbf{A}^* \mathbf{K} \mathbf{B} (\mathbf{R} + \mathbf{B}^{\text{th}} \mathbf{K} \mathbf{B})^{-1} \mathbf{B}^* \mathbf{K} = 0.$$

The optimal value of $J(\tilde{\mathbf{x}}_0, \tilde{u})$ is given by the following equation

$$J(\tilde{\mathbf{x}}_0, \tilde{u}) = \tilde{\mathbf{x}}_0^* \mathbf{P} \tilde{\mathbf{x}}_0,$$

where $\mathbf{P} = \mathbf{K}$ is the solution of discrete algebraic Riccati equation.

3.2. Optimal Control of Reduced-Order Model

3.2.1. Optimal Control Without Constraints

From the unconstrained optimal feedback control problem of the above full-order model (11), the equations of the reduced-order model are as follows:

$$\begin{cases} \tilde{\alpha}(k+1) = \mathbf{A}_r \tilde{\alpha}(k) + \mathbf{B}_r \tilde{u}(k), \\ \tilde{y}(k) = \mathbf{c}_r \tilde{\alpha}(k). \end{cases} \quad (12)$$

And the objective function is

$$\min_{\tilde{u}} J = \sum_0^{\infty} (\tilde{\alpha}^{\text{th}} \mathbf{Q} \tilde{\alpha} + \tilde{u}^* R \tilde{u}).$$

where $\mathbf{Q} = \mathbf{c}_r^* \mathbf{c}_r$ and $\tilde{\alpha} = \alpha - \alpha_f$.

Feedback Controller based on LQR is

$$\tilde{u}(k) = -\mathbf{L} \tilde{\alpha}(k), \mathbf{L} = (\mathbf{R} + \mathbf{B}_r^{\text{th}} \mathbf{K} \mathbf{B}_r)^{-1} \mathbf{B}_r^* \mathbf{K} \mathbf{A}_r,$$

and \mathbf{K} is determined by the following algebraic Riccati equation

$$-\mathbf{K} + \mathbf{Q} + \mathbf{A}_r^{\text{th}} \mathbf{K} \mathbf{A}_r - \mathbf{A}_r^* \mathbf{K} \mathbf{B}_r (\mathbf{R} + \mathbf{B}_r^{\text{th}} \mathbf{K} \mathbf{B}_r)^{-1} \mathbf{B}_r^* \mathbf{K} \mathbf{A}_r = 0.$$

3.2.2. Optimal Control with Constraints

The states are assumed to be unconstrained while the control input is constrained by

$$u_{\min} \leq \tilde{u}_k \leq u_{\max} \text{ for } k \geq 0 \text{ with } u_{\min} < 0 < u_{\max}. \quad (13)$$

Constrained infinite-horizon LQR problem

$$J(\tilde{\alpha}_0, \tilde{u}) = \min_{\tilde{u}} \sum_0^{\infty} (\tilde{\alpha}_k^{\text{th}} \mathbf{Q} \tilde{\alpha}_k + \tilde{u}_k^* R \tilde{u}_k), \quad (14)$$

subject to reduced order model (12) and $u_{\min} \leq \tilde{u}_k \leq u_{\max}$ for $\forall k \in \mathbb{Z}^*$.

Due to the incorporation of an infinite-horizon and under the assumptions of unconstrained stability and detectability as well as $\mathbf{Q} = \mathbf{Q}^* \geq \mathbf{0}$ and $R > 0$, this method can guarantee nominal stability as long as the optimal cost is finite, i.e.

$$J(\tilde{\alpha}_0, \tilde{u}) < \infty \Rightarrow \lim_{k \rightarrow \infty} \tilde{\alpha}_k \rightarrow \mathbf{0}.$$

As shown in (14), the constrained infinite-horizon LQR

$$\begin{aligned} J_N[\tilde{\alpha}_0, \tilde{u}] &= \min_{\tilde{u}} \sum_0^{\infty} (\tilde{\alpha}_k^{\text{H}} \mathbf{Q} \tilde{\alpha}_k + \tilde{u}_k R \tilde{u}_k) \\ &= \min_{\tilde{u}} \left[\sum_0^{N-1} (\tilde{\alpha}_k^{\text{H}} \mathbf{Q} \tilde{\alpha}_k + \tilde{u}_k R \tilde{u}_k) + \sum_N^{\infty} (\tilde{\alpha}_k^{\text{H}} \mathbf{Q} \tilde{\alpha}_k + \tilde{u}_k R \tilde{u}_k) \right] \\ &= \min_{\tilde{u}_k} \sum_0^{N-1} (\tilde{\alpha}_k^{\text{H}} \mathbf{Q} \tilde{\alpha}_k + \tilde{u}_k R \tilde{u}_k) + \tilde{\alpha}_N^{\text{T}} \mathbf{P} \tilde{\alpha}_N, \end{aligned} \tag{15}$$

subject to (12) with $\tilde{\alpha}(t_f) = 0$ and

$$u_{\min} \leq \tilde{u}_k \leq u_{\max} \text{ for } 0 \leq k \leq N-1.$$

Note that $\mathbf{P} = \mathbf{K}$ is the solution to the discrete algebraic Riccati equation. In order to ensure the stability of the finite-horizon system, the equality constraint of the terminal state of $\tilde{\alpha}(t_f) = 0$ is added to the finite-horizon receding the optimization problem, and t_f is sufficiently large.

In the above optimization problem, when the control time domain N of the quadratic control problem is large, the computational cost of solving the corresponding quadratic programming problem is large. The calculation is complex, and the computational complexity is exponentially related to N .

In this paper, CSROA can solve the model quickly and reduce the huge computational cost. At the same time, the online state feedback optimization control of constrained quadratic optimization problem can be obtained at all times.

Based on the linear properties of the system, then

$$\tilde{\alpha}(k) = \mathbf{A}_r^k \tilde{\alpha}(0) + \sum_{j=0}^{k-1} \mathbf{A}_r^j \mathbf{B} \tilde{u}_{k-1-j}, \quad k = 1, 2, \dots, N. \tag{16}$$

Combined with equation (15) and equation (16), one can obtain the following optimization problems in the standard form of quadratic programming

$$J = \frac{1}{2} \tilde{\alpha}(0)^{\text{H}} \mathbf{Y} \tilde{\alpha}(0) + \min_{\tilde{u}} \left(\frac{1}{2} \tilde{\mathbf{U}}_N^{\text{H}} \mathbf{H} \tilde{\mathbf{U}}_N + \mathbf{F} \tilde{\mathbf{U}}_N \right), \tag{17}$$

subject to

$$u_{\min} \leq \tilde{\mathbf{U}}_N \leq u_{\max},$$

where $\mathbf{H} = \mathbf{H}^*$, \mathbf{H} , \mathbf{F} , \mathbf{Y} can be obtained from \mathbf{Q} , \mathbf{R} in (15).

For optimal decision variable $\tilde{\mathbf{U}}_N(\tilde{\alpha}_0) = (\tilde{u}_0, \dots, \tilde{u}_{N-1})^*$, we adopt CSROA of quadratic programming with $N = 1$, and the same optimal control solution performed depends on the updated variable $\tilde{\alpha}(0)$ at each sampling time.

results in an insoluble infinite-dimensional optimization problem. However, by using the optimality principle, (14) can be recast into the following constrained finite-horizon linear quadratic regulation problem

It has shown that the saturated LQR control sequence is equivalent to a receding horizon control sequence of the solution to (16) with no terminal state inclusion condition and with $N = 1$ as well as (14) holds and Hessian matrix $\nabla_{u_i, u_j}^2 J_N(\tilde{\alpha}_0, \tilde{u}) \geq 0$, see reference [17].

Then the algorithm with input constraints based on ISLQR controller is as follows

Step 1. Input an initial state value $\tilde{\alpha}(0)$, compute the optimal control input from LQR control $\tilde{u}(k) = -\mathbf{L} \tilde{\alpha}(k)$;

Step 2. Verify the extreme value of the following formula (18),

$$\tilde{u} = \begin{cases} u_{\min}, & \text{if } \tilde{u}(k) < u_{\min}, \\ \tilde{u}(k), & \text{if } u_{\min} \leq \tilde{u}(k) \leq u_{\max}, \\ u_{\max}, & \text{if } \tilde{u}(k) > u_{\max}. \end{cases} \tag{18}$$

Then use quadratic controller $\tilde{u}(k) = -\mathbf{L} \tilde{\alpha}(k)$ for optimal control.

Step 3. Return to Step 2 to continue iterative validation until the end state equality constraint $\tilde{\alpha}(t_f) = \mathbf{0}$ is finally met, such that $\tilde{u} = 0$.

4. Numerical Simulations

All the parameters in the numerical simulation are shown in Table 1, and all computing is based on PC computers with Intel (R) Core (TM) i7-4790 CPU with frequency of 3.60 GHz and random access memory of 8GB. The concentration output of the reactor is controlled from steady state 0.05 to steady state 0.55. And all simulation results are obtained by MATLAB.

Table 1. Parameter selection in numerical simulation.

$v_1 = v_2$	D	m	$Dx = Dy$	Dt
1	0.01	50	0.06	0.008

In the case of unconstrained control, for the open-loop simulation ($u(x, t) \equiv 0.2$), the spatial and temporal distribution of concentration is shown in Figure 1 by using the parameters in Table 1. The concentration increases monotonously in spatial and temporal, and it takes some time

to reach the steady state value.

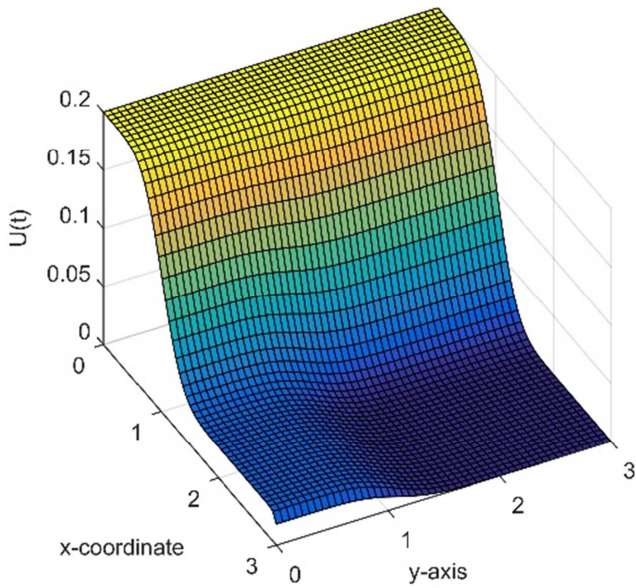


Figure 1. Spatial and temporal distribution of concentration $U(x, y, t)$.

In closed-loop simulation, when the uncertain weights are respectively taken as 0.06, 0.3, 0.6, the corresponding optimal input and output is shown in Figures 2 and 3. For the same control value R , the control effect of full-order model (11) with $r = 2499$ and reduced-order model (12) with $r = 25$ is the same. The larger the value of R , the smaller the input u and the smaller the output overshoot y . Compared with open-loop control, the optimal feedback control of closed-loop is faster, more accurate and more stable when $u = u_f$. The CPU time taken for full-order model (11) and reduced-order model (12) is shown in Table 2, and it can be observed that when the control effect is the same, the reduced-order model saves computational time greatly.

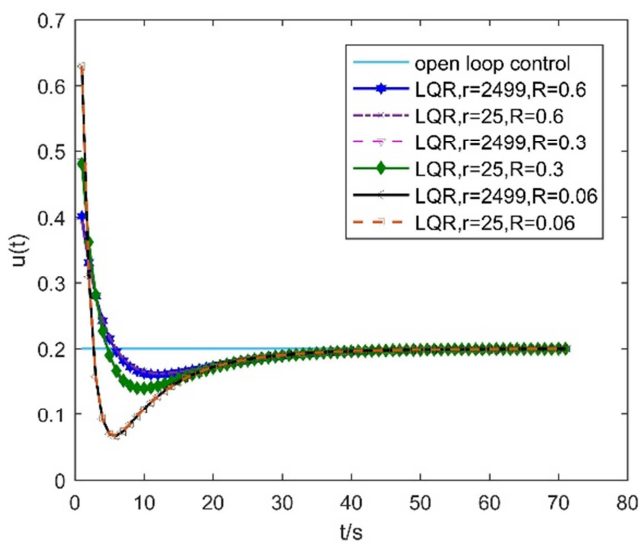


Figure 2. Optimal input for unconstrained transition process.

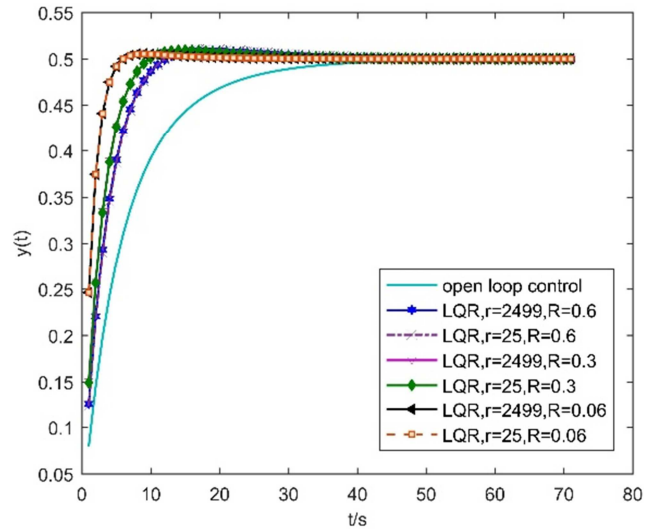


Figure 3. Optimal output for unconstrained transition process.

Table 2. Computing time under the same control effect.

R	Full-order model (s)	Reduced-order model (s)
0.06	3012.8	2.5274
0.3	2991.8	2.2548
0.6	3305.6	1.6955
Open loop	0.6253	0.03561

Took constraints into account, when the input constraint $0 \leq u \leq 0.4$, the state constraint $\tilde{\alpha}(t_f) = 0$ and R is respectively taken as 0.013, 0.6, the input and output of the optimal feedback control for reduced-order model (12) is shown in figures 4 and 5.

From the control effect of LQR controller without constraints (12), CSROA (17) and ISLQR controller (18), it can be seen that the optimal feedback control effect of the three methods is the same when $R = 0.6$. When $R = 0.013$, the error between the value of control move produced by the ISLQR and the value obtained by the unconstrained LQR control law is defined as $\square u_k = \tilde{u} - \tilde{u}(k)$. This error result is the same as that of Marjanovic et al. [17], which further proves the effectiveness of the proposed method.

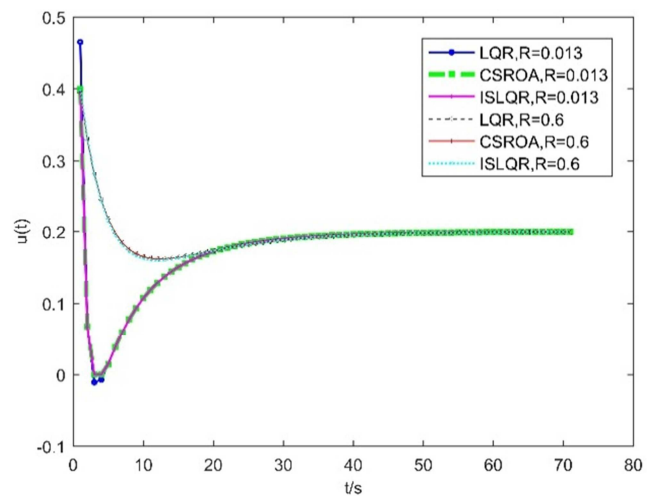


Figure 4. Optimal input for constrained transition process.

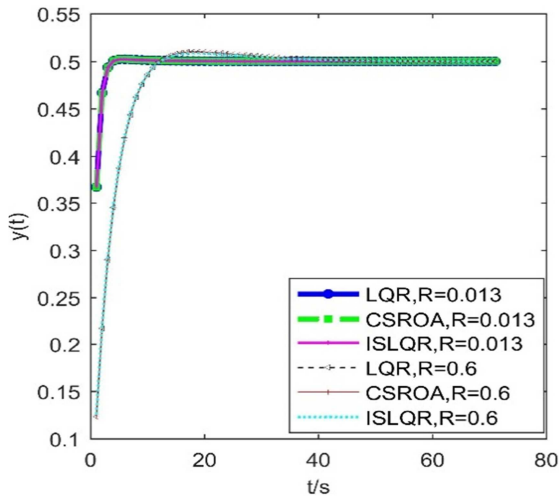


Figure 5. Optimal output for constrained transition process.

In the case of constraints, the input and output of the optimal feedback control of ISLQR are shown in figures 6 and 7, respectively. It can be seen that the optimal input and corresponding output of the reduced-order model and the full-order model are the same under the constraint conditions. For the same value R , the control effect is same too.

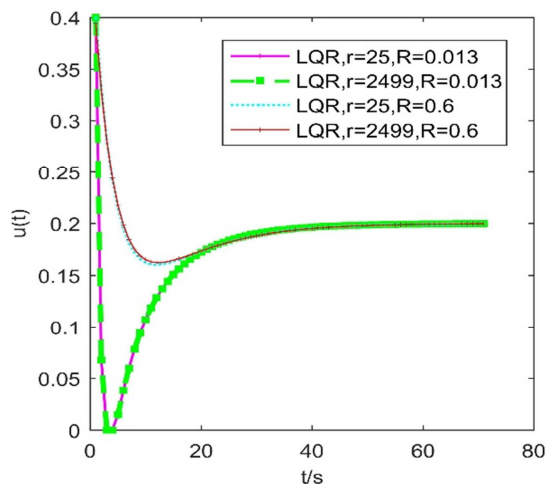


Figure 6. Constrained full-order and reduced-order optimal input.

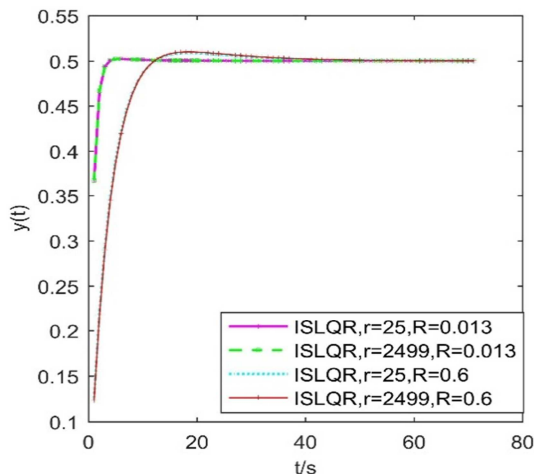


Figure 7. Constrained full-order and reduced-order optimal output.

It can be seen from Table 3 that the optimal control CPU time of the reduced order model with constraint conditions is much less than that of the full-order model, which fully proves the high efficiency of the reduced-order model.

Table 3. Computing time under the constraint conditions.

R	Full-order model (s)	Reduced-order model (s)
0.06	4757.5	3.0754
0.013	4540.4	3.3927

5. Conclusion

In this paper, a real-time controller is designed for reduced-order model (12) by reducing the order of the full-order model (11) with the POD method, CSROA and ISLQR controller, which simplifies the solution of the two-dimensional unsteady convection-diffusion boundary control problem with constraints.

The method of reducing order model designed in our paper can improve the efficiency of calculation and optimization. The full-order model [2499-order, in (11)] needs to solve 2,499 equations at each time step, and the reduced-order model [25-order, in (12)] only needs to solve 25 equations, and the control effect is same. To a large extent, the computation memory and CPU computing time are saved.

On the other hand, a real-time online predictive optimal feedback controller based on a low-order model is designed, which provides a simple control method for solving the low-order model optimal control problem.

Fund

This work was supported by the National Natural Science Foundation of China (grant number 11461013).

References

- [1] Buske D, Vilhena M T, Tirabassi T, et al. Air pollution steady-state advection-diffusion equation: the general three-dimensional solution [J]. Journal of Environmental Protection. 2012, 03 (09): 1124-1134.
- [2] Tirabassi T, Vilhena M T, Buske D, et al. An analytical air pollution model with time dependent eddy diffusivity [J]. Journal of Environmental Protection. 2013, 04 (08): 16-23.
- [3] Costa C, Vilhena M, Moreira D, et al. Semi-analytical solution of the steady three-dimensional advection-diffusion equation in the planetary boundary layer [J]. Atmospheric Environment. 2006, 40 (29): 5659-5669.
- [4] Stavre R. A distributed control problem for two coupled fluids in a porous medium [J]. SIAM Journal on Control and Optimization. 2015, 53 (1): 313-335.
- [5] Saasen A, Hodne H. The influence of vibrations on drilling fluid rheological properties and the consequence for solids control [J]. Applied Rheology. 2016, 26 (2).
- [6] Prins M W, Welters W J, Welters J W. Fluid control in multichannel structures by electrocapillary pressure [J]. Science. 2001, 291 (5502): 277-280.

- [7] Chen X B. Modeling and control of fluid dispensing processes: a state-of-the-art review [J]. *International Journal of Advanced Manufacturing Technology*. 2009, 43 (3-4): 276-286.
- [8] Zhang G, Zhu D, Qiu X, et al. Skeleton-based control of fluid animation [J]. *Visual Computer International Journal of Computer Graphics*. 2011, 27 (3): 199-210.
- [9] Zhao Y, Schultz N E, Truhlar D G. Design of density functionals by combining the method of constraint satisfaction with parametrization for thermochemistry, thermochemical kinetics, and noncovalent interactions. [J]. *Journal of Chemical Theory & Computation*. 2006, 2 (2): 364.
- [10] Zhu M, Marínez S. On distributed convex optimization under inequality and equality constraints [J]. *IEEE Transactions on Automatic Control*. 2011, 57 (1): 151-164.
- [11] Andreani R, Birgin E G, Martínez J M, et al. On augmented lagrangian methods with general lower-level constraints [J]. *Siam Journal on Optimization*. 2007, 18 (4): 1286-1309.
- [12] Belhachmi Z, Sacépée J M, Sokolowski J. Mixed finite element methods for smooth domain formulation of crack problems [J]. *SIAM Journal on Numerical Analysis*. 2005, 43: 1295-1320.
- [13] G Y, D W, Ha D. Adaptive finite difference for seismic wavefield modelling in acoustic media [J]. *Scientific Reports*. 2016, 6: 30302.
- [14] Wu G C, Baleanu D, Zeng S D. Finite-time stability of discrete fractional delay systems: Gronwall inequality and stability criterion [J]. *Communications in Nonlinear Science & Numerical Simulations*. 2018, 57.
- [15] Yang L, Yan H, Liu H, et al. Optimal implicit staggered-grid finite-difference schemes based on the sampling approximation method for seismic modeling [J]. *Geophysical Prospecting*. 2016, 64 (3): 595-610.
- [16] Rapún M L, Vega J E. Reduced order models based on local POD plus Galerkin projection [J]. *Journal of Computational Physics*. 2010, 229.
- [17] Marjanovic, Ognjen, Lennox, et al. Minimising conservatism in infinite-horizon LQR control [J]. *Systems & Control Letters*. 2002, 46 (4): 271-279.
- [18] Li M, Christofides P D. Optimal control of diffusion-convection-reaction processes using reduced-order models [J]. *Computers & Chemical Engineering*. 2008, 32 (9): 2123-2135.